

Continuous Wave Nanowire Lasing

Robert Röder,^{*,†} Marcel Wille,[†] Sebastian Geburt,[†] Jura Rensberg,[†] Mengyao Zhang,[‡] Jia Grace Lu,[‡] Federico Capasso,[§] Robert Buschlinger,^{||} Ulf Peschel,^{||} and Carsten Ronning[†]

[†]Institut für Festkörperphysik, Friedrich-Schiller-Universität Jena, Max-Wien-Platz 1, 07743 Jena, Germany

[‡]Department of Physics and Astronomy, University of Southern California, Los Angeles, California 90089, United States

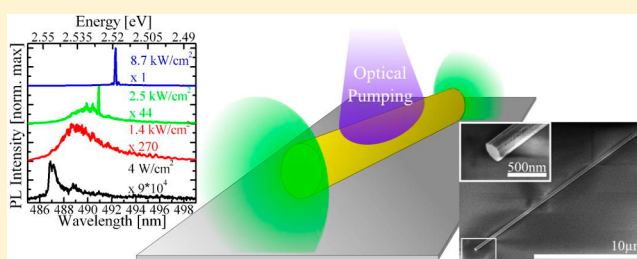
[§]School of Engineering and Applied Science, Harvard University, Cambridge, Massachusetts 02138, United States

^{||}Institut für Optik, Information und Photonik, Friedrich-Alexander-Universität, 91058 Erlangen, Germany

S Supporting Information

ABSTRACT: Tin-doped cadmium sulfide nanowires reveal donor–acceptor pair transitions at low-temperature photoluminescence and furthermore exhibit ideal resonator morphology appropriate for lasing at continuous wave pumping. The continuous wave lasing mode is proven by the evolution of the emitted power and spectrum with increasing pump intensity. The high temperature stability up to 120 K at given pumping power is determined by the decreasing optical gain necessary for lasing in an electron–hole plasma.

KEYWORDS: CdS nanowires, VLS growth, doping, DAP transition, continuous wave laser emission



The forthcoming limitations of conventional electronic integrated circuits promote reinforced work in nanophotonics, as on-chip optical data processing and transmission can overcome the drawbacks of electrical interconnects and boost performance.¹ Semiconductor nanowires are promising building blocks for on-chip optoelectronic components, as they are functional and connecting units in both photonics and electronics and offer highly localized light emission² as well as efficient waveguiding.^{3,4} In addition, semiconductor nanowires mark the lower physical size limit of multimode photonic laser systems,⁵ making them ideal nanoscale light sources for optical data transmission and processing in a spectral range that is determined by the direct band gap of the material. Cadmium sulfide (CdS) nanowires offer a strong optical mode confinement⁶ and make the green spectral range around 2.4 eV accessible as Fabry–Pérot nanolasers with remarkable low thresholds at room temperature, but yet only in pulsed mode operation.⁷ Thus, further improvement for future integration in optoelectronic devices will be gained by nanoscaled continuous wave (cw) coherent light sources. Although an electrically driven super luminescent nanowire light source and amplified spontaneous emission was demonstrated,²⁵ laser oscillations from subwavelength nanostructures via optical carrier injection have been so far only observed at pulsed excitation,^{5,8,9} as high pumping power is necessary to establish the population inversion responsible for gain and light amplification due to the high threshold values for lasing of nanowires. The nature of the pulsed excitation allows the introduced thermal budget to dissipate to the supporting substrate during the off times and therefore prevents the nanowires being degraded.

In this study, we will address the optimized fabrication that circumvents the pretreatment of the growth substrate with catalyst deposition for the synthesis of high-quality Sn doped CdS nanowires with shallow levels. We will clearly prove intense cw laser emission at low temperatures from such high-quality, long, and straight nanowire resonators. A detailed discussion of the gain mechanisms and temperature-dependent measurements elucidate the creation of electron–hole plasma at the established excitation conditions.

Tin-doped CdS nanowires were synthesized in a horizontal tube furnace by chemical vapor deposition method. A mixture of CdS, SnO, SnO₂, and graphite powder with a molar ratio of 1:1:1:0.1 was evaporated as the source material at 1000 °C in the center of a horizontal tube furnace and transported by Ar carrier gas at 1 atm for 40 min downstream toward silicon growth substrates. SnO and SnO₂ were reduced to Sn by carbon at 600 °C during a previous heating step, which subsequently catalyzed the growth of wurtzite CdS nanowires. The as-synthesized CdS nanowires, which reveal an excellent crystal quality (more details on TEM analysis can be found in Supporting Information S1), have lengths up to 100 μm and diameters from 50 nm to several micrometers. Further details of the growth process will be submitted in another paper by the co-workers of this work.²⁷ The Sn content in the CdS nanowires presented here was determined by EDX to be 1–3 at. % (see Supporting Information S2). Single nanowires were

Received: April 16, 2013

Revised: June 21, 2013

Published: July 17, 2013



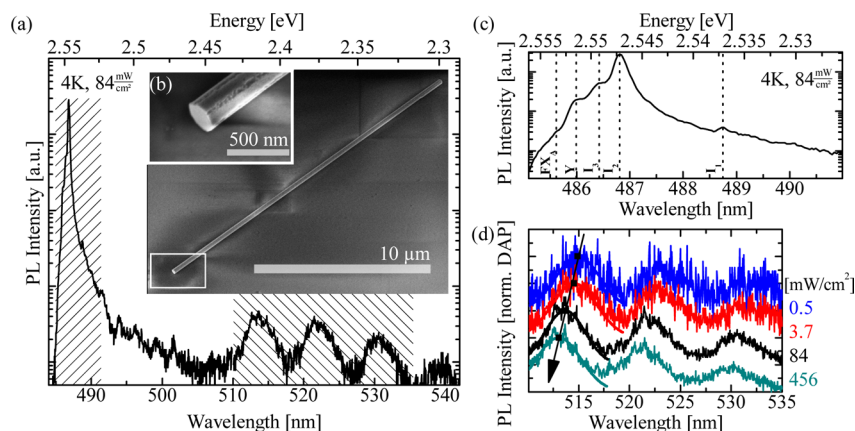


Figure 1. (a) Microphotoluminescence (μ PL) spectrum of a single CdS:Sn nanowire at 4 K originating from the excitation spot shows near band edge emission (NBE) (485–491 nm), phonon replica of NBE transitions (490–505 nm), and the donor–acceptor pair transition (DAP) accompanied by LO phonon replica (510–540 nm). (b) Scanning electron microscopy (SEM) image of the respective CdS:Sn nanowire (diameter \sim 300 nm, length 19.9 μ m) with smooth end facets lying on a SiO₂/Si substrate well suited as a nanowire laser resonator. (c) Streaked μ PL NBE spectrum of (a) with assigned excitonic emission lines. (d) μ PL spectra showing the blue shift of the DAP transition from low (0.5 mW/cm²) to moderate excitation conditions (456 mW/cm²), as depicted by the arrow.

transferred on top of clean SiO₂/Si substrates by dry imprint for subsequent microphotoluminescence (μ PL) measurement using a home-built epi-fluorescence setup.^{7,26} The thermally grown low refractive index SiO₂ layer with a 1.5 μ m thickness ensures the strong optical mode confinement in the nanowire waveguide, thereby avoiding largely the leakage of electromagnetic power into the substrate as well as the energy dissipation out of the nanowire optical cavity. The nanowire samples were mounted in a Janis ST-500 liquid He flow cryostat with incorporated heating unit to apply cryostat temperatures between $T = 4$ K and room temperature. A HeCd pumping laser (325 nm, cw) was focused by a 36 \times reflective microscope objective (NA = 0.5) to a spot size of 20 μ m² for the excitation of single nanowires. Their luminescence light was collected by the same objective, dispersed by a 500 mm monochromator, and detected with a liquid nitrogen cooled CCD. The laser power was determined behind the microscope objective using a Si diode power meter and subsequently corrected by the area of the laser focus spot to determine the excitation density.

Optically excited single CdS:Sn nanowires show photoluminescence at the position of the excitation spot as well as slightly weaker emission out coupled from the nanowire cavity at their end facets due to efficient waveguiding.¹⁰ Figure 1a shows the low-temperature emission spectrum from the excitation spot of a Sn-doped CdS nanowire, whose morphology is shown in the scanning electron microscopy (SEM) image in Figure 1b. The nanowire emits an intense near band edge luminescence. The near band edge spectral region between 485–491 nm is shown in detail in Figure 1c. It reveals several distinct PL features caused by free and bound excitonic recombinations. The emission line at 485.6 nm can be attributed to recombinations of free intrinsic A excitons (FX_A).¹¹ The more intense 485.9 nm emission line (labeled Y in Figure 1c) was also detected by Thomas and Hopfield,¹¹ but the origin is unclear. The emission labeled I₃ at 486.3 nm is caused by excitons bound to ionized donors and the very strong emission line I₂ at 486.8 nm by excitons bound to neutral donors. Thus, n -type doping of the CdS nanowires is very likely since this donor bound excitonic emission exceeds the emission of acceptor bound excitons (labeled I₁) at 488.6 nm by 2 orders

of magnitude. However, the incorporated Sn with its amphoteric nature in CdS introduces also an emission band around 513 nm accompanied by longitudinal optical (LO) phonon replica with an energetic spacing of 38 meV. This band is usually attributed to direct donor–acceptor pair transitions (DAP)^{13,14} and is absent in pure undoped CdS nanowires.^{7,12} The DAP emission energy is given by

$$E_{\text{DAP}} = E_{\text{g}} - (E_{\text{D}} + E_{\text{A}}) + \frac{e^2}{4\pi\epsilon\epsilon_0 r} \quad (1)$$

where E_{g} is the CdS band gap energy, while $E_{\text{D(A)}}$ is the activation energy of the donor (acceptor) and the last term is the electron–hole Coulomb interaction energy. The experimental evidence for a DAP transition as origin of the emission band can therefore be obtained by the power-dependent emission spectra at $T = 4$ K presented in Figure 1d. The spectra reveal a clear blue shift of \sim 10 meV with increasing excitation density by a factor of 900. This blue shift appears since the mean distance r of the involved donor–acceptor pairs decreases with carrier concentration as the excitation power is increased. The observation of acceptor bound excitons as well as of DAP recombination, which are both not seen for undoped CdS nanowires (see Supporting Information S3), suggest together with the above observations that amphoteric and shallow levels are introduced into the band gap by the incorporation of Sn, with clearly dominant n -type character.

Power-dependent PL spectra of the waveguided emission originating from the nanowire facet end are shown in Figure 2a. Only spontaneous emission of the I₂ and I₁ lines emerge from the nanowire end at low cw excitation powers below several hundred W/cm². The bound excitonic emission is here efficiently waveguided along the nanowire cavity. The new line at 487.1 nm, which is next to the I₂ line, is not present in the previous spectrum due to lower excitations and can be attributed to the formation of biexcitons in direct band gap CdS,¹⁵ whose recombination cause the red shift of the so-called M band by 8 meV relatively to the FX_A emission.¹⁶ The M band broadens at moderate excitation powers, accompanied by a shift to lower energies and subsequent saturation in the high excitation regime above 1 kW/cm². The broad asymmetric emission band between 488 and 493 nm occurs above 1 kW/cm²

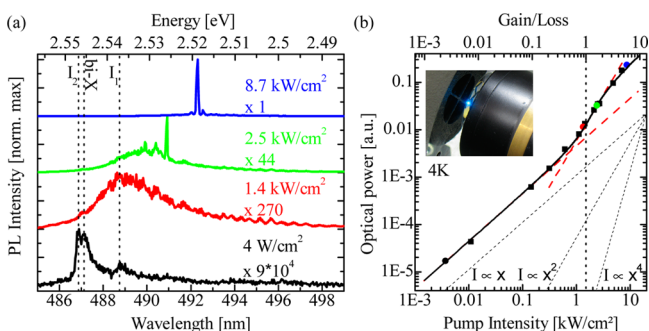


Figure 2. (a) The μ PL end facet spectra of the respective nanowire presented in Figure 1b at 4 K show the spontaneous NBE emission and the biexciton emission at moderate cw excitation of 4 W/cm². Above 1 kW/cm² the spectrum is broadened and red-shifted accompanied by intensity modulations indicating standing waves in the Fabry–Pérot type resonator. At higher excitations above 2 kW/cm², sharp, equidistant longitudinal laser modes evolve superimposed to broadened emission. Red-shifted modes dominate the emission spectra at very high excitation above 6 kW/cm². (b) The s-shaped power dependence in the log–log plot of the integrated PL intensity data versus pump power clearly proves cw lasing in single CdS:Sn NW by fitting the data with a model developed for multimode laser oscillators¹⁷ (solid line) with fitting parameter $\alpha_0 = 0.16$. The dotted lines labeled $I \propto x$ (x^2 , x^4) should guide the eye to linear (quadratic, to the power of four) dependence. The inset shows the bright cw emission from the single nanowire visible with unaided eye.

cm² excitation as a result of efficient waveguiding superimposed with intensity modulations, which indicate standing electromagnetic waves in the nanowire resonator.¹⁰ At the low energy site above 493 nm, where the modulations are more clearly visible, the propagating waves experience a more pure photonic character due to the low absorption in this region.

If the excitation is increased above 2 kW/cm², sharp and equidistant modes evolve superimposed to the broad spontaneous emission at the low energy side of the asymmetric emission band. The dominant modes shift further to lower energies of around 492.3 nm as pumping increases, while the spontaneous emission becomes negligible. Figure 2b presents the optical power emitted from one single nanowire facet end as a function of the pump intensity. The experimental data reveal a S-shape in the double-logarithmic plot. The linear power dependence obtained in the low excitation regime attributed to spontaneous emission below 1 kW/cm² fades to a superlinear increase accompanied by evolving sharp modes, which is interpreted as the onset of amplified spontaneous emission (ASE). The power dependence returns to a linear slope above ~ 6 kW/cm², at which the sharp modes dominate the spectra. The evolution of the emitted spectrum and the emitted power with pump intensity unambiguously prove continuous wave laser action² in single CdS:Sn nanowires with low lasing threshold of ~ 2 kW/cm² and is consistent with the Casperson model for multimode laser emission.¹⁷ This threshold value is below the so far reported room temperature lasing thresholds of ~ 10 kW/cm² for CdS and ~ 300 kW/cm² for ZnO nanowire oscillators at pulsed excitation.²⁷ The cw emission from one single nanowire is extremely bright and can be even seen at ambient light by the unaided eye, like it is demonstrated in the inset of Figure 2b.

Nanowire coherent light sources gain benefits from continuous wave operation mode and need also to operate at higher temperatures for practical applications. To explore the

temperature dependence, macro PL is measured on a CdS:Sn nanowire growth ensemble sample (see Supporting Information S4). The I₂ and I₁ emission lines show the most intense PL emission intensity similar to the end facet spectra of the single nanowire. Both emissions vanish around $T = 60$ K due to the dissociation of the excitons from the shallow defects, whereas the free exciton emission increases around 487 nm. We determined the values of the Varshni shift¹⁸ of the excitonic emission for our samples from these measurements. This behavior is plotted in Figure 3a, together with the temperature-

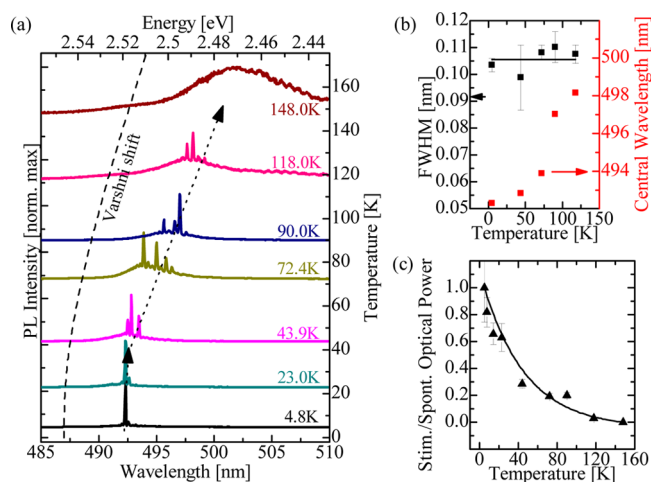


Figure 3. (a) End facet μ PL spectra reveal the temperature stability of cw lasing up to 120 K at 9 kW/cm². The lasing modes shift to lower energies with increasing temperature as pointed by the arrow. A broadening of the gain profile enveloping the modes is obtained. (b) The FWHM of the most prominent lasing modes remains constant as temperature increases, while the central wavelength red shifts. (c) The decreasing ratio of stimulated to spontaneous emission indicating gain in the optically pumped NW is fitted as a guide to the eyes as a function of temperature. The lasing modes and the underlying broad spontaneous emission of the spectra in (a) were fitted using Gaussian functions to obtain the intensity ratio $I_{\text{stim.}}/I_{\text{spont.}}$ as a function of temperature.

dependent lasing performance of the single CdS:Sn nanowire at constant pump intensity of 9 kW/cm². The baseline of the spectra is arranged at the corresponding measured cryostat temperature in this plot. Up to $T = 25$ K, the shift of the lasing modes is nearly negligible, while above $T = 40$ K a distinct red shift appears, which is accompanied by a strong broadening of the gain profile with an increasing number of modes at the low energy side. The evaluated central wavelength of the lasing modes and their width are plotted in Figure 3b. A similar red shift was demonstrated for the gain spectra caused by an electron–hole plasma in CdS crystals.¹⁹ The cw lasing keeps an efficient level up to a temperature of 120 K at the given and constant pump intensity, which is also evident from the low full width at half maximum (FWHM) of the sharp modes. As the extracted FWHM value of about 0.1 nm remains constant up to 120 K (Figure 3b), this indicates that the stimulated emission cannot be attributed to exciton related gain, since the FWHM would otherwise increase in such a case.¹⁰ The decrease of the optical gain as a function of temperature is determined by the ratio of stimulated optical power to the amount of underlying spontaneous emission, as plotted in Figure 3c. At low temperatures, the lasing modes dominate the spectra, while around 120 K, only low-intensity modes superimposed to the

spontaneous emission are present indicating amplified spontaneous emission (ASE). The gain value in the EHP of CdS declines from 5 to 50 K by a factor of ~ 3 ,¹⁹ which is in good agreement with the observed behavior in Figure 3c. The mode spacing of the lasing modes fits the relation for a Fabry–Pérot type resonator of 19.9 μm nanowire length at all evaluated temperatures.

Four possible mechanisms have been proposed to explain the optical gain in highly excited CdS crystals. For inelastic exciton–exciton (X–X) scattering (P_n band), in which the decaying exciton recombines emitting a photon and scatters another exciton into higher branches,²⁰ gain values up to 160 cm^{-1} are estimated.¹⁵ The X–LO scattering and the X–electron scattering mechanism would only contribute to gain at elevated temperatures above 75 K and above 100 K with higher thresholds than X–X gain.^{6,20,21} Thus, we do not consider these processes as contributing to gain in our samples, in addition to the fact that the spectral position particularly that of the X–LO scattering mechanism at 492.9 nm does not fit to the observed lasing modes in our experiments. The lasing of CdS and ZnO nanowires occurring at room temperature and pulsed excitation was attributed to gain achieved in an electron–hole plasma (EHP),^{5,7,22} while low-temperature pulsed lasing in CdS nanowires was considered to be caused by X–X scattering.⁶

The red shift of the lasing modes in Figure 2a at high excitations results most likely from the band gap renormalization as an effect of high charge carrier densities in the electron–hole plasma (EHP), while exciton related emissions would not shift.²³ Temperature effects could also induce the energy shift of lasing modes at high excitations. However, the temperature needed to cause a red shift of more than 1.3 nm would be higher than 60 K, when the excitation is increased from 2.5 kW/cm^2 to 8.7 kW/cm^2 (compare with Varshni shift above) and would lead to an additional broadening of the gain profile, as shown in Figure 3b, which is not present in Figure 2a. The heating of the nanowire under continuous pumping was estimated to be only ~ 35 K by increasing the excitation by 4 orders of magnitude from 0.1 W/cm^2 to 1.2 kW/cm^2 (see Supporting Information S5). Therefore, we can rule out an increasing temperature to have a remarkable impact to the observed lasing mode shift. Furthermore, only the formation of an EHP is likely to reach enough optical gain g in CdS for lasing, as values up to $2.5 \times 10^4 \text{ cm}^{-1}$ have been reported.¹⁹ The modal gain g_{mod} needs crucially to exceed the losses in the nanowire: $g_{\text{mod}} = \Gamma \cdot g > \alpha_w + \alpha_m$, where Γ is the confinement factor, α_w the waveguide losses, and α_m the losses at the mirror-like end facets: $\alpha_m = 1/L \ln(1/R_{1,2})$, with L being the nanowire length and R the power reflectivity.⁵ Assuming that the optical mode propagates completely confined within the investigated CdS:Sn nanowire cavities resulting in $\Gamma \sim 1$ and $\alpha_w \ll \alpha_m$, we can thus simplify $g > 1/L \ln(1/R_{1,2})$ for lasing. Since the lower nanowire length limit for photonic lasing was estimated to be 7 μm , and $R_{1,2}$, which depends on the transversal mode, does not exceed 0.5,²⁴ the required gain value is in the order of $g > 10^3 \text{ cm}^{-1}$. Thus, the formation of an EHP is the exclusive mechanism providing the necessary optical gain to overcome the threshold for nanowire lasing at low temperatures as well as at room temperature.¹⁹

In recent studies on unintentional doped CdS nanowires synthesized via conventional VLS using Au as catalyst,⁷ we also observe cw lasing at low temperatures as well. The benefit of the optimized fabrication process using Sn catalysts remains

therefore in circumventing the pretreatment of the growth substrate and in the conformal tin doping. Excellent crystal quality and optimal resonator morphology sufficient for cw lasing is reached using both fabrication methods. An absolute upper temperature limit for cw lasing will be determined by the weakened gain and therefore required high pumping intensities, which then again accounts for the heating problem. A proper solution for high temperature cw lasing can be provided by enhancing the reflectivity at the end facets in order to lower the threshold.

In conclusion, we have demonstrated successful tin doping of CdS nanowires that incorporates shallow and amphoteric levels within the band gap with a dominating n -type character. The high quality of the material together with the high quality nanowire resonators show extreme low lasing threshold values, enabling continuous wave (cw) lasing at temperatures below 120 K. The optical gain mechanism is most likely caused by an electron–hole plasma upon high pumping powers.

■ ASSOCIATED CONTENT

📄 Supporting Information

Supporting Figures including a high-resolution TEM image of the crystal lattice of the investigated CdS:Sn NWs, EDX spectrum of a single tin-doped CdS NW, typical PL spectrum of an imprinted ensemble of undoped CdS nanowires, temperature-dependent PL spectra of a CdS:Sn NW growth ensemble, and μPL spectra of a single CdS:Sn NW, plus the estimation of charge carrier density. This material is available free of charge via the Internet at <http://pubs.acs.org>.

■ AUTHOR INFORMATION

✉ Corresponding Author

*E-mail: robert.roeder@uni-jena.de.

Notes

The authors declare no competing financial interest.

■ ACKNOWLEDGMENTS

The authors gratefully acknowledge funding by the German Research Society (DFG) within the project FOR1616. J.G.L. and M.Y.Z. would like to thank the support of Prof. Robert Hellwarth, and the work on synthesis and structure characterization is part of the Center for Energy Nanoscience funded by the U.S. Department of Energy, Office of Science, EFRC program under Award Number DE-SC0001013.

■ REFERENCES

- (1) Huang, Y.; Duan, X.; Lieber, C. *Small* **2005**, *1*, 142–147.
- (2) Zimmler, M. A.; Bao, J.; Capasso, F.; Müller, S.; Ronning, C. *Appl. Phys. Lett.* **2008**, *93*, 051101–3.
- (3) Pan, A.; Liu, R.; Yang, Q.; Zhu, Y.; Yang, G.; Zou, B.; Chen, K. J. *Phys. Chem B* **2005**, *109*, 24268–24272.
- (4) Voss, T.; Svacha, G.; Mazur, E.; Müller, S.; Ronning, C.; Konjhodzic, D.; Marlow, F. *Nano Lett.* **2007**, *7*, 3675–3680.
- (5) Zimmler, M. A.; Capasso, F.; Müller, S.; Ronning, C. *Semicond. Sci. Technol.* **2010**, *25*, 024001–12.
- (6) Agarwal, R.; Barrelet, C. J.; Lieber, C. M. *Nano Lett.* **2005**, *5*, 917–920.
- (7) Geburt, S.; Thielmann, A.; Röder, R.; Borschel, C.; McDonnell, A.; Kozlik, M.; Kühnel, J.; Sunter, K. A.; Capasso, F.; Ronning, C. *Nanotechnology* **2012**, *23*, 365204–6.
- (8) Johnson, J. C.; Choi, H.-J.; Knutsen, K. P.; Schaller, R. D.; Yang, P.; Saykally, R. J. *Nat. Mater.* **2002**, *1*, 106–110.
- (9) Piccione, B.; Cho, C.-H.; van Vugt, L. K.; Agarwal, R. *Nat. Nanotechnol.* **2012**, *7*, 640–645.

- (10) van Vugt, L. K.; Piccione, B.; Cho, C.-H.; Aspetti, C.; Wirshba, A. D.; Agarwal, R. *J. Phys. Chem. A* **2011**, *115*, 3827–3833.
- (11) Thomas, D. G.; Hopfield, J. J. *Phys. Rev.* **1962**, *128*, 2135–2148.
- (12) Leite, R. C. C.; Scott, J. F.; Damen, T. C. *Phys. Rev. Lett.* **1969**, *22*, 780–782.
- (13) Henry, C. H.; Faulkner, R. A.; Nassau, K. *Phys. Rev.* **1969**, *183*, 798–806.
- (14) Xu, X.; Zhao, Y.; Sie, E. J.; Lu, Y.; Liu, B.; Ekahana, S. A.; Ju, X.; Jiang, Q.; Wang, J.; Sun, H.; Sum, T. C.; Huan, C. H. A.; Feng, Y. P.; Xiong, Q. *ACS Nano* **2011**, *5*, 3660–3669.
- (15) Levy, R.; Grun, J. B. *Phys. Status Solidi A* **1974**, *22*, 11–38.
- (16) Shionoya, S.; Saito, H.; Hanamura, E.; Akimoto, O. *Solid State Commun.* **1973**, *12*, 223–226.
- (17) Casperson, L. W.; Lunnam, S. D. *Appl. Opt.* **1975**, *14*, 1193–1199.
- (18) Varshni, Y. *Physica* **1967**, *34*, 149–154.
- (19) Bohnert, K.; Schmieder, G.; El-Dessouki, S.; Klingshirn, C. *Solid State Commun.* **1978**, *27*, 295–299.
- (20) Koch, S. W.; Haug, H.; Schmieder, G.; Bohnert, W.; Klingshirn, C. *Phys. Status Solidi B* **1978**, *89*, 431–440.
- (21) Haug, H.; Koch, S. *Phys. Status Solidi B* **1977**, *82*, 531–543.
- (22) Versteegh, M. A. M.; Vanmaekelbergh, D.; Dijkhuis, J. I. *Phys. Rev. Lett.* **2012**, *108*, 157402–5.
- (23) Klingshirn, C. F. *Semiconductor Optics*, 2nd ed.; Springer: New York, 2005.
- (24) Maslov, A. V.; Ning, C. Z. *Appl. Phys. Lett.* **2003**, *83*, 1237–1239.
- (25) Duan, X.; Huang, Y.; Agarwal, R.; Lieber, C. M. *Nature* **2003**, *421*, 241–245.
- (26) Geburt, S. Ph.D. Thesis, University of Jena, Jena, Germany, 2013; <http://www.db-thueringen.de/servlets/DocumentServlet?id=22078>
- (27) Zhang, M.; Wille, M.; Röder, R.; Geburt, S.; Zhu, Z.; Huang, L.; Heedt, S.; Schapers, T.; Ronning, C.; Lu, J. G. *Nano Research* **2013**, to be submitted.